

MODELING THE ONE-STAGE SYNTHESIS OF COMPOSITE PARTICLES OF THE NUCLEUS–SHELL TYPE IN SEPARATE OXIDATION OF TITANIUM AND SILICON TETRACHLORIDES IN A PLASMACHEMICAL REACTOR

S. M. Aulchenko^{a,b} and E. V. Kartaev^a

UDC 532.075.8

The authors have modeled the one-stage synthesis of titania and silica composite nanoparticles in the working zone of a plasmachemical reactor by the chloride method based on separate oxidation of titanium and silicon tetrachlorides with pre-mixing of the reagents by bubbling. Within the framework of the developed synthesis model, the authors have obtained data on the size of the nuclei of the composite particles, the shell thickness, and the ratio of the number of shell-coated and uncoated particles.

Keywords: *titania, silica, composite particles, plasmachemical reactor, single-velocity multicomponent medium, homogeneous and heterogeneous reactions, coagulation.*

Introduction. One of the most promising trends in modern technologies is the synthesis of nanocomposite powders of oxide ceramics, which belong to a novel class of materials with the possibility of controlling their physicochemical properties depending on the purpose. In particular, wide use has been enjoyed by nanosize particles of titania TiO_2 . Here, in many practical applications, it is required that the photocatalytic activity of TiO_2 particles be suppressed, e.g., in additives of pigmented titania to dyes and to plastic and during the production of paper and the production of sunscreens. In this case it is required that the area of the photoactive free surface of titania be as small as possible, with the optical properties of the material itself being preserved. This requirement is satisfied by, e.g., $\text{TiO}_2 + \text{SiO}_2$ nanocomposite particles of the "nucleus–shell" structure; here, the greater the thickness of the SiO_2 amorphous layer and the lower its microporosity, the more depressed the photoactivity of a composite nanopowder [1]. In [2], El-Toni et al. modeled for the first time the one-stage synthesis of $\text{TiO}_2 + \text{SiO}_2$ composite particles in the working zone of a plasmachemical reactor by the chloride method based on separate oxidation of titanium and silicon tetrachlorides. The use of plasmatrons is a promising trend in creating high-capacity units for nanomaterial production [3, 4]. Here, the concentration of components in the mixed reagents fed to the reactor was not tied to a concrete mode of mixing. Furthermore, the range of the flow rates of the air and silicon–tetrachloride mixture allowed a temperature reduction to values below 1200 K, at which chlorosiloxanes $(\text{SiO}_x\text{Cl}_y)_n$ can be formed, in the zone of mixing with the central jet [5], and no constraint on the minimum thickness of formation of a shell was imposed in the model.

In the present work, we give results of the modeling of the one-stage synthesis of $\text{TiO}_2 + \text{SiO}_2$ composite nanoparticles by the chloride method based on separate oxidation of titanium and silicon tetrachlorides, which was carried out with account of these factors.

Formulation of the Problem. A diagram of the working zone of a flow-type reactor is shown in Fig. 1 (the actual position is vertical). A nitrogen jet with temperature T_1 and flow rate Q_1 flows into the working zone via a channel. A mixture of titanium tetrachloride and air at the temperature T_2 and flow rate Q_2 is fed via the first lateral slot. In the mixing zone, there is the reaction to form first the gas-phase component of TiO_2 and next TiO_2 particles. Thereafter, as the particles move along the reactor, we have their growth due to the surface reaction and coagulation. Results of the calculations and experiments of this stage are given in [6, 7]. A mixture of silicon tetrachloride and air at the temperature T_3 and with flow rate Q_3 is fed via the second lateral slot.

In the mixing fuel, we have a homogeneous reaction to form a SiO_2 gas-phase component which condenses on titania particles and a homogeneous reaction to form a solid phase on the surface of both TiO_2 particles and $\text{TiO}_2 + \text{SiO}_2$ composite

^aS. A. Khristianovich Institute of Theoretical and Applied Mechanics, 4/1 Institutskaya Str., Novosibirsk, 630090, Russia; email: aultch@itam.nsc.ru; ^bNovosibirsk State University of Architecture and Civil Engineering, 159 Turgenev Str., Novosibirsk, 630008, Russia. Translated from Inzhenerno-Fizicheskii Zhurnal, Vol. 93, No. 1, pp. 114–119, January–February, 2020. Original article submitted March 25, 2019.

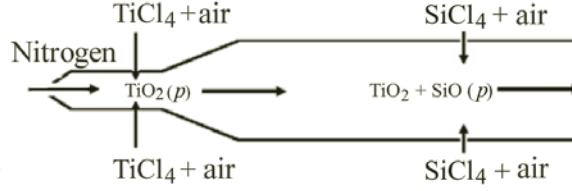
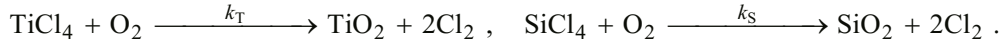


Fig. 1. Diagram of the working zone of the flow-type reactor.

particles. In contrast to the model of [2], in the model employed in the present work, we calculate in advance the mass of the SiO_2 solid phase whose formation is possible in any calculated volume and the area that may be coated by it as a layer of thickness no smaller than the diameter of SiO_2 monomers. As a result we determine the fraction of particles of which the layer of silica particles is formed. In the presence of the titania particles and composite particles alike in the computational cell, these fractions are proportional to the number of particles of each type. The next step in generalizing the model will be the inclusion of the possibility of being partially coated. The degree of adequacy of each version of the model will be checked experimentally on a laboratory setup whose operating parameters correspond to the parameters adopted in calculations. Also, we will check the assumption that there is no coagulation of the composite particles.

Mathematical Model. Consideration is given to the flow of a viscous heat-conducting mixture of gases. The components of the mixture are O_2 , N_2 , TiCl_4 , SiCl_4 , TiO_2 , SiO_2 , and Cl_2 . The last three components result from the generalized chemical reactions



We consider a single-fluid regime of flow which is modeled using a system of quasi-gasdynamics equations [6]. With account of external forces and heat sources, this system is of the form

$$\frac{\partial \rho}{\partial t} + \text{div } \mathbf{j} = 0,$$

$$\frac{\partial \rho \mathbf{u}}{\partial t} + \text{div } (\mathbf{j} \otimes \mathbf{u}) + \nabla p = \rho \mathbf{F} + \text{div } \Pi, \quad (1)$$

$$\frac{\partial E}{\partial t} + \text{div } (\mathbf{j}H) + \text{div } \mathbf{q} = (\mathbf{j} \cdot \mathbf{F}) + \text{div } (\Pi \cdot \mathbf{u}) + Q.$$

The vector of the mass-flux density is determined by the following relation:

$$\mathbf{j} = \rho \mathbf{u} - \tau [\text{div } (\rho \mathbf{u} \otimes \mathbf{u}) + \nabla p - \rho \mathbf{F}], \quad \tau = \frac{M}{\text{ReSc}} \frac{T}{p}.$$

To this system are added the continuity equations for the mixture's components

$$\frac{\partial \rho_i}{\partial t} + \text{div } \mathbf{j}^i = \sum_j J^{(ji)} \quad (2)$$

and the volume concentration of the solid phase

$$\frac{\partial c_p}{\partial t} + \text{div } (c_p \mathbf{u}) = \sum_j J^{(jp)}. \quad (3)$$

On the right-hand sides of Eqs. (2) and (3), account has been taken of the following kinetic relations describing a variation in the concentrations of titanium tetrachloride and titania in the gas and solid phases, and also silicon tetrachloride and silica in the gas and solid phases due to the homogeneous and heterogeneous reactions and to the phase transition:

$$\begin{aligned}\frac{dC^1}{dt} &= -k_1^T C^1 = -(k_1^g + k_1^s A) C^1, & \frac{dC^2}{dt} &= k_1^g C^1 - k_1^p C^2, \\ \frac{dC^3}{dt} &= k_1^s C^1 A + k_1^p C^2, & \frac{dC^4}{dt} &= -k_5^T C^4 = -(k_5^g + k_5^s A) C^4, \\ \frac{dC^5}{dt} &= k_5^g C^4 - k_5^p C^5, & \frac{dC^6}{dt} &= k_5^s C^4 A + k_5^p C^5.\end{aligned}\quad (4)$$

Supplementary relations closing the system of equations are of the form

$$p = \rho R_m T \frac{m_g}{1 - c_p}, \quad \alpha_i = \rho_i / \rho, \quad R_m = R_g \left(\sum_i \alpha_i / m_i \right).$$

If to relations (1)–(4) is added the equation for the number of titania particles

$$\frac{dN}{dt} = k_1^g C^1 N_{Av} - \frac{\beta N^2}{2}, \quad (5)$$

with account taken of their initial d_0 and knowing the mass of the particles and their number and volume concentration at each instant of time in each computational cell, we can calculate their size.

The coagulation parameter according to [5] was calculated from the formula

$$\beta = 8\pi d_B d_p \left[\frac{d_p}{d_p + g\sqrt{2}} + \frac{4d_B\sqrt{2}}{u_p d_p} \right]^{-1},$$

where $g = \left(\frac{1}{3d_p l_a} \right) \left[(d_p + l_a)^3 - (d_p + l_a)^2 \right] - d_p$, $l_a = \frac{8d_B}{\pi u_p}$, and $d_B = \frac{3\sqrt{mkT/2\pi}}{2\rho d_p^2 (1 + \alpha\pi/8)}$.

Boundary Conditions. On the reactor walls, there are the adhesion conditions, the absence of the heat flux, and the equality of the normal derivative of pressure to zero (this supplementary condition is caused by the special properties of the quasi-hydrodynamic system). The flow rate and temperature are assigned for the jets. To calculate the values of pressure, density, and velocity at the input boundaries of the jets, use is made of the boundary conditions based on the use of the Riemann invariants for Euler equations.

In integrating Eqs. (1)–(3) numerically, they are written in a cylindrical coordinate system (the problem is axisymmetric) and are reduced to a dimensionless form. We select, as the basic dimensional parameters, the channel radius, and also the velocity of sound of the air which is at rest at a temperature of 300 K in the reactor at the initial instant of time and the air density.

To numerically solve the system of equations, use is made of a difference scheme explicit in time. Time derivatives are approximated by forward differences with the first order of accuracy. Space derivatives are approximated by central differences with the second order of accuracy.

Calculation Results. The basic series of calculations whose results can be verified with experimental data was carried out in the following formulation. In the first step, we calculated a quasi-stationary flow field in the reactor, which was formed by injecting a jet from a plasmatron. Thereafter, the injection of lateral jets occurred.

The geometric characteristics of the reactor were as follows: $L_R = 444$ mm, $d_R = 32$ mm, $L_C = 38$ mm, $d_C = 7$ mm, $L_{Tr} = 33$ mm, and $\alpha = 15^\circ$. The coordinates of the midlines of the slots for injecting lateral jets were $z_1 = 28$ mm and $z_2 = 292$ mm.

The parameters of the setup were $T_1 = 4500$ K, $Q_1 = 1$ g/s, $T_2 = 300$ K, $Q_2 = 2.5$ g/s, $T_3 = 300$ K, and $Q_3 = 0.8$ – 1 g/s. The composition of the first lateral jet was as follows: air 99.5% and $TiCl_4$ 0.5%, and the composition of the second lateral jet, air 99.2% and $SiCl_4$ 0.8%.

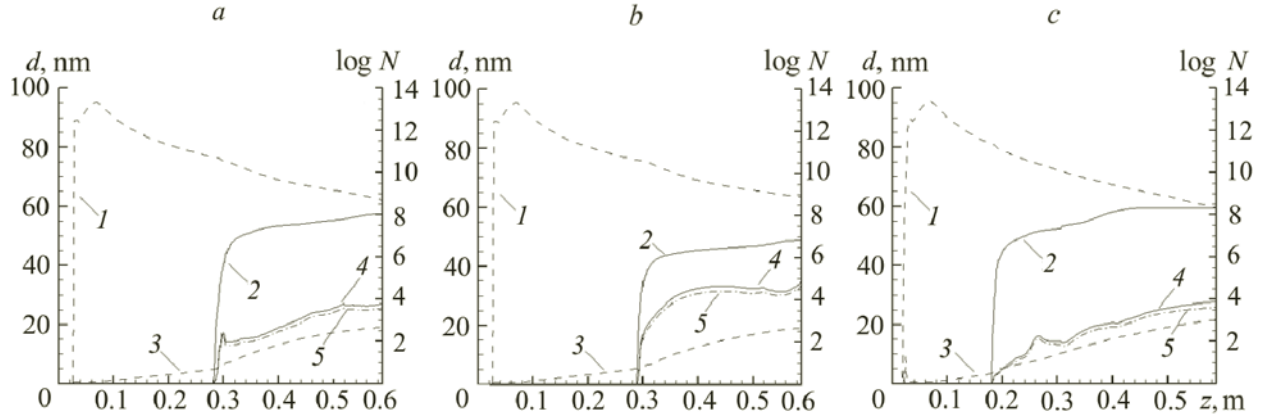


Fig. 2. Distribution of the weighted-mean diameters of particles and of the logarithm of the density of the number of particles: a) calculation at $z_2 = 292$ mm and $Q_3 = 1$ g/s; b) calculation at $z_2 = 292$ mm and $Q_3 = 0.8$ g/s; and c) calculation at $z_2 = 192$ mm and $Q_3 = 0.8$ g/s; 1) logarithm of the TiO_2 -particle number density, 2) logarithm of the composite particle number density, 3) diameter of TiO_2 particles, 4) diameter of composite particles, and 5) diameter of the nucleus of composite particles.

The assigned values of constants in Eqs. (4) and (5) according to [8, 9] were as follows:

$$k_{\text{T}}^{\text{r}} = 8.26 \cdot 10^4 \exp\left(\frac{-10,681}{T}\right), \quad k_{\text{T}}^{\text{s}} = 4.9 \cdot 10^3 \exp\left(\frac{-8993}{T}\right), \quad k_{\text{T}}^{\text{p}} = 1.2 \cdot 10^{10} \exp\left(\frac{-10,681}{T}\right), \quad (6)$$

$$k_{\text{S}}^{\text{r}} = 8.0 \cdot 10^{14} \exp\left(\frac{-400,000}{T}\right), \quad k_{\text{S}}^{\text{s}} = 4.0 \cdot 10^{13} \exp\left(\frac{-40,828}{T}\right), \quad k_{\text{S}}^{\text{p}} = k_{\text{T}}^{\text{p}}.$$

Figure 2 gives the distributions of the weighted-mean diameters of particles along the reactor by their number $d_i = \frac{1}{N_i} \sum_j d_{ij} N_{ij}$, $N_i = \sum_j N_{ij}$ and the distribution of the logarithm of the density of the number of particles at different values of the flow rate of the mixture of air and a silicon-tetrachloride vapor and different locations of the slot. It can be seen from Fig. 2 that at the reactor outlet, there are two kinds of nanoparticles: titania particles and composite particles whose nuclei are comprised of titania, and the shell, of silica.

The calculations show that the ratio of the number of particles depends on both the relation of the flow rates of the jets Q_2 and Q_3 (Fig. 2a and b) and the position of a slot via which the mixture of air and a silicon-tetrachloride vapor is injected (Fig. 2a and c). The size of the composite particles and the thickness of the shell depend on the same parameters. In addition to the reduction in the mass of the silicon oxide synthesized in the gas phase, decrease in the flow rate Q_3 results in a reduction in the dimension of the region in which the shell is formed. Since this region is adjacent to the reactor wall, titania particles larger than cross-section average ones are found to be in it. This is because of the smaller velocity of the flow near the walls and, accordingly, the increase in the time during which TiO_2 particles grow due to the surface reaction and coagulation. For example, the diameters of the nucleus of a composite particle and of the entire particle in the versions presented in Fig. 2a and b are equal to 25.58 and 27.06 and to 36.15 and 37.28 nm respectively. The upstream displacement of the slot for injecting the mixture of air and silicon tetrachloride increases the time during which the shell is formed; this has an effect on the number of composite particles at exit and the shell thickness alike. Thus, even with a decrease of 20% in the flow rate Q_3 in the version presented in Fig. 2c compared to the version in Fig. 2a, the number of composite particles has grown and amounts to 40% of the total number of particles at exit (in the version in Fig. 2a, the composite particles amount to 20% of the total number of particles). The shell thickness in versions a, b, and c is equal to 1.5, 1.2, and 1.7 nm respectively.

Conclusions. On the basis of separate oxidation of titanium and silicon tetrachlorides, we have modeled the one-stage synthesis of titania and silica composite nanoparticles of the "nucleus–shell" structure in the working zone of a plasmachemical reactor. The flow rate of the precursors and their fractions in the gas mixtures introduced by lateral jets into the reactor's working zone correspond to the parameters that can be obtained with pre-mixing of the reagents by bubbling. It is precisely these parameters that will be basic in checking the employed physicomathematical model of particle synthesis experimentally. Furthermore, the obtained calculation results enable us to experimentally check the influence of regime parameters of the setup on both the general particle size and the shell thickness.

Acknowledgments. This work was carried out within the framework of the Program of Basic Scientific Research of State Academies of Science for the Years 2013–2020 (project AAAA-A17-117030610120-2) and with partial support from the Russian Foundation for Basic Research (Grant No. 18-08-00219a).

NOTATION

A , relative area of particles, cm^2/cm^3 ; C^1 , C^2 , C^3 , C^4 , C^5 , and C^6 , concentrations of titanium tetrachloride, titania in the gas phase and titania in the solid phase, silicon tetrachloride, silica in the gas phase, and silica in the solid phase, mole/ cm^3 ; c_p , volume concentration of the solid phase; d_B , diffusion coefficient of a Brownian particle, m^2/s ; d_C and d_R , diameters of the channel and the reactor, mm; d_p , diameter of particles, nm; d_0 , initial diameter of particles, nm; d_i , weighted mean diameter of a particle in the i th cross section, nm; d_{ij} , diameter of a particle in the j th computational cell of the i th cross section, nm; E , normalized total energy of a unit volume; \mathbf{F} , normalized vector of the mass-force density; H , normalized total specific enthalpy; $J^{(ij)}$, normalized intensity of mass conversion of the j th component into the i th one in a unit volume of the mixture; \mathbf{j} , normalized vector of the mixture's mass-flux density; \mathbf{j}^i , normalized vector of the mass-flux density of the i th component; k_T^r and k_S^r , rates of generalized reactions, 1/s; k , Boltzmann constant, J/K; k_T^g and k_S^g , rates of homogeneous reactions, 1/s; k_T^s and k_S^s , rates of surface reactions, cm/s; k_T^{ph} and k_S^{ph} , rates of phase transitions, cm^3/s ; L_C , L_R , and L_T , lengths of the channel, the reactor, and the transition tube, mm; M , Mach number; m , mass of a carrier-gas molecule; m_g , mass fraction of the gas; M_i , mass of particles in the i th cross section; m_i , molecular weight of the i th component; m_{ij} , mass of particles in the j th computational cell of the i th cross section; N , number of particles in a unit volume, N_{Av} , Avogadro number; N_i , number of particles in the i th cross section; N_{ij} , number of particles in the j th computational cell of the i th cross section; N_2 , nitrogen; O_2 , oxygen; p , normalized pressure; Q , normalized heat; Q_1 , rate of flow of a nitrogen jet from the plasmatron, g/s; Q_2 and Q_3 , rates of flow of the first and second lateral jets, g/s; Re , Reynolds number; R_g , specific gas constant, J/(kg·K); R_m , specific gas constant of the mixture, J/(kg·K); SiCl_4 , silicon tetrachloride; SiO_2 , silica; Sc , Schmidt number; t , times, s; T , normalized temperature; T_1 , temperature of a nitrogen jet from the plasmatron, K; T_2 and T_3 , temperatures of the lateral jets, K; TiCl_4 , titanium tetrachloride; TiO_2 , titania; \mathbf{u} , normalized velocity vector of the mixture; u_p , velocity of particles, m/s; z , axis of the cylindrical coordinate system; z_1 and z_2 , coordinates of the midlines of slots for injection of lateral jets, mm; α , accommodation coefficient; α^0 , slope of the transition tube, deg; α_i , mass fraction of the i th component; β , coagulation parameter, cm^3/s ; Π , normalized viscous-stress tensor; ρ , normalized density of the mixture; ρ_i , normalized density of the i th component; τ , normalized relaxation parameter. Subscripts: C, channel; g, gas; m, mixture; p, particles; s, surface; S, silicon; T, titanium; Tr, transition; R, reactor; r, reaction.

REFERENCES

1. A. M. El-Toni, S. Yin, and T. Sato, Control of silica shell thickness and microporosity of titania–silica core–shell type nanoparticles to depress the photocatalytic activity of titania, *J. Colloid Interface Sci.*, **300**, No. 1, 123–130 (2006).
2. S. M. Aulchenko and E. V. Kartaev, Numerical simulation of the synthesis of titania–silica composite nanoparticles in plasmachemical reactor, *AIP Conf. Proc.* 2027, 04002 (2018); <https://doi.org/10.1063/1.5065276>.
3. S. A. Zhdanok, I. F. Buyakov, A. V. Krauklis, and K. O. Borisevich, On the formation of carbon nanostructures on the steel surface of a reactor as a result of the decomposition of hydrocarbons in the low-temperature plasma, *J. Eng. Phys. Thermophys.*, **82**, No. 3, 407–413 (2009).
4. S. A. Zhdanok, I. F. Buyakov, A. V. Krauklis, A. N. Laktyushin, K. O. Borisevich, and M. V. Kiyashko, Obtaining carbon nanomaterials in a plant with a plasma generator and a working zone of rectangular cross section, *J. Eng. Phys. Thermophys.*, **83**, No. 1, 6–9 (2010); <https://elibrary.ru/contents.asp?id=34345230>.

5. T. Giesenberg, S. Hein, M. Binnewies, and G. Kickelbick, Synthesis and functionalization of a new kind of silica particle, *Angew. Chem. Int. Ed.*, **43**, 5697–5700 (2004).
6. S. M. Aulchenko, Controlling the process of titanium dioxide nanoparticle growth in a continuous-flow plasma-chemical reactor, *J. Eng. Phys. Thermophys.*, **86**, No. 5, 1027–1034 (2013).
7. E. V. Kartaev, V. P. Lukashov, S. P. Vashenko, S. M. Aulchenko, O. B. Kovalev, and D. V. Sergachev, Experimental study of the synthesis of the ultrafine titania powder in plasmachemical flow-type reactor, *Int. J. Chem. React. Eng.*, **12**, No. 1 (2014); DOI: 10.1515/ijcre-2014-0001.
8. A. Kolesnikov and J. Kekana, Nanopowders production in the plasmachemical reactor: modelling and simulation, *Int. J. Chem. React. Eng.*, **9**, Article A83 (2011).
9. H. K. Park and K. Y. Park, Control of particle morphology and size in vapor-phase synthesis of titania, silica and alumina nanoparticles, *KONA Powder Particle J.*, No. 32, 85–101 (2015).